Evidence for $SrHo_2O_4$ and $SrDy_2O_4$ as model J_1-J_2 zigzag chain materials

A. Fennell,[1,*] V. Y. Pomjakushin,[1] A. Uldry,[2] B. Delley,[2] B. Prévost,[3] A. Désilets-Benoit,[3] A. D. Bianchi,[3] R. I. Bewley,[4] B. R. Hansen,[5] T. Klimczuk,[6,7] R. J. Cava,[8] and M. Kenzelmann[9]

[1]*Laboratory for Neutron Scattering, Paul Scherrer Institute, CH-5232 Villigen, Switzerland*
[2]*Condensed Matter Theory Group, Paul Scherrer Institut, CH-5232 Villigen PSI, Switzerland*
[3]*Département de Physique & Regroupement Québécois sur les Matériaux de Pointe (RQMP), Université de Montréal, Montréal, Québec, Canada H3C 3J7*
[4]*ISIS Facility, Rutherford Appleton Laboratory, Chilton, Didcot OX11 0QX, United Kingdom*
[5]*Department of Physics, Technical University of Denmark, DK-2800 Lyngby, Denmark*
[6]*Faculty of Applied Physics and Mathematics, Gdansk University of Technology, Narutowicza 11/12, PL-80-233 Gdansk, Poland*
[7]*Institute of Physics, Pomeranian University, Arciszewskiego, PL-76-200 Slupsk, Poland*
[8]*Department of Chemistry and Princeton Materials Institute, Princeton University, Princeton, New Jersey 08544, USA*
[9]*Laboratory for Development and Methods, Paul Scherrer Institut, CH-5232 Villigen PSI, Switzerland*

(Received 20 December 2013; published 17 June 2014)

Neutron diffraction and inelastic spectroscopy is used to characterize the magnetic Hamiltonian of $SrHo_2O_4$ and $SrDy_2O_4$. Through a detailed computation of the crystal-field levels we find site-dependent anisotropic single-ion magnetism in both materials, and diffraction measurements show the presence of strong one-dimensional spin correlations. Our measurements indicate that competing interactions of the zigzag chain, combined with frustrated interchain interactions, play a crucial role in stabilizing spin-liquid type correlations in this series.

DOI: 10.1103/PhysRevB.89.224511 PACS number(s): 75.10.Pq, 75.10.Dg, 75.30.Gw

I. INTRODUCTION

Geometrically frustrated magnetic materials have proven to be a fertile area of condensed matter research. Competition between interactions can lead to macroscopic degeneracies and novel states of matter with emergent properties, providing "toy models" for statistical mechanics and examples of exotic quasiparticle excitations. A prime example are the rare-earth titanates in which the combination of the rare-earth ion-dependent crystal-field anisotropy and a highly frustrated lattice produce a rich array of novel magnetic materials with both classical and quantum spin-liquid phases [1,2].

SrR_2O_4 belongs to a recently discovered family of geometrically frustrated rare-earth materials that features nontrivial ground states [3–7]. The rare-earth sites (R) form a honeycomb in the ab plane [Fig. 1(a)] and a triangular ladder along the c axis [Fig. 1(b)]. $SrHo_2O_4$ was shown to have a one-dimensionally (1D) correlated state at low temperatures, with moments that lie along either the b or c axes [7], whereas $SrDy_2O_4$ shows only short-range order and weak diffuse scattering [3]. In this paper, we will demonstrate, first, that the two rare-earth sites feature a strong anisotropy pointing along the b or c axes, respectively, and second, that $SrDy_2O_4$ features one-dimensional correlations with up-up-down-down local order, but remains disordered on long length scales to the lowest measured temperatures. We argue that the magnetism in SrR_2O_4 can be mapped on to the Ising J_1-J_2 spin chain model, and that the competing interactions of this model play a crucial role in the stabilization of the spin-liquid state in $SrDy_2O_4$ [8–10].

The relation between the ladder structure and the J_1-J_2 model can be understood from Fig. 1, where the rungs and legs correspond to the J_1 and J_2 interactions, respectively. Theory predicts that in $S = \frac{1}{2}$ systems with antiferromagnetic J_1, when $J_2 > J_1/2$, the ground state changes from a simple antiferromagnetic Néel, $\uparrow\downarrow\uparrow\downarrow$, state to an up-up-down-down, $\uparrow\uparrow\downarrow\downarrow$, double Néel configuration [8,11]. On the application of a magnetic field the system enters an up-up-down phase, seen as a $\frac{1}{3}$ magnetization plateau at $H = -J_1/2 + J_2$ and finally saturates into a ferromagnetic phase, when $H = J_1 + J_2$, in which all of the moments are aligned with the applied magnetic field [9,11,12]. A $\frac{1}{3}$ plateau is also found for classical moments, when the moments are strongly Ising like [10]. Despite several examples of Heisenberg J_1-J_2 [13–15], and J_1 Ising [16–18], materials, there are few previous examples that meet the criteria for the Ising J_1-J_2 chain model [19], and ones that can test the phase diagram at the classical limit are still needed.

The SrR_2O_4 crystallographic structure is described by the $Pnam$ space group, and each unit cell contains a total of eight R atoms that are divided into two inequivalent $4c$ sites ($4c_1$ and $4c_2$) at the center of distorted, edge-sharing, oxygen octahedra [Fig. 1(b)] [3]. The $4c_1$ and $4c_2$ sites form separate zigzag chains, with rung interactions $J_{1_{c1}}$ and $J_{1_{c2}}$, and leg interactions $J_{2_{c1}}$ and $J_{2_{c2}}$. The interchain coupling is mediated by the J_3 and J_4 pathways, which combine with the J_1 pathways to give a distorted honeycomb lattice in the ab plane [Fig. 1(a)]. The R ions have a monoclinic site symmetry and the free ion ground state of the R atoms is split into the maximum possible number of levels. For the $^5I_8$, Ho^{3+} ion, with an integer value for J, we expect $2J + 1 = 17$ singlets and for the $^6H_{15/2}$, Dy^{3+}, with a half integer value for J, the site symmetry gives rise to $J + 1/2 = 8$ doublets [20]. Magnetization studies suggest that each of the sites, in both the Ho and Dy materials, have large single-ion anisotropies, with b and c easy-axis directions [5]. The measured entropy indicates that the Dy moments have $S = \frac{1}{2}$ degrees of freedom [21].

*amy.poole@psi.ch

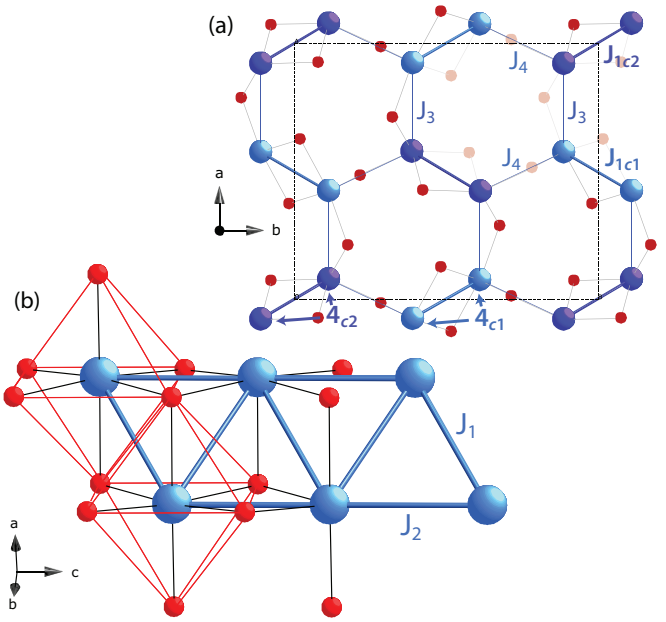

FIG. 1. (Color) The structure of $SrDy_2O_4$. The $4c_1$ and $4c_2$ sites are dark and light blue and oxygen is shown in red, respectively, with (a) showing the hexagonal arrangement of the atoms in the *ab* plane, and (b) the Dy_{4c1} ladder structure with the J_1-J_2 exchange pathways [3].

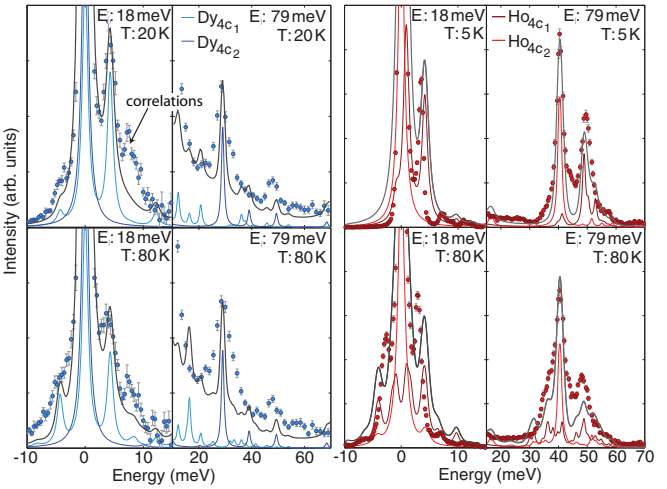

FIG. 2. (Color) Inelastic neutron powder data for $SrDy_2O_4$ (blue, left) and $SrHo_2O_4$ (red, right) measured on HET. The calculated fits for the individual sites are shown with thin solid lines and their average, convoluted with the instrument resolution is shown in thick gray [22]. An instrumental background was added to the Dy data.

II. RESULTS

A. Crystal field excitations

To determine the crystal-field excitations and determine the magnetic single-ion anisotropies, inelastic neutron scattering experiments were performed on powder samples of $SrDy_2O_4$ and $SrHo_2O_4$ prepared by the method described in Ref. [3]. The inelastic neutron spectra of the Dy compound were recorded with an incident energy $E_i = 18$, 79, and 117 meV at temperatures of $T = 20$, 50, and 80 K, on the HET time-of-flight spectrometer, ISIS. The Ho compound was measured with an incident energy of $E_i = 18$, 70, and 79 meV at temperatures of $T = 5$, 50, 80, and 150 K on the HET spectrometer (Fig. 2). Due to the low symmetry of ion sites the excitations were modeled using a point charge calculation, [23] which capture the intra-atomic electrostatic interactions, the spin-orbit coupling, and the effect of the crystal electric field. Fits to spectra on the meV energy scale are insensitive to the electrostatic and spin-orbit coupling, so only the crystal-field scaling factor $S_{\rm xtal}$ was refined. The values found for $SrDy_2O_4$ are $S^{4c1}_{\rm xtal} = 0.35$ and $S^{4c2}_{\rm xtal} = 0.53$, whereas for the Ho analog we find $S^{4c1}_{\rm xtal} = 0.62$ and $S^{4c2}_{\rm xtal} = 0.70$. As $S_{\rm xtal}$ is dependent on the orbital overlap or covalency of the atom, the less-than-one scaling values may mean a significant f-orbital contraction is taking place, and/or the charges allocated to ions (Dy^{3+}, Ho^{3+}, Sr^{2+}, O^{2-}) are overestimated. The fits show that the first excited states of the Dy^{3+} crystal-field levels are found at 4 and 29 meV above the ground state doublet for the $4c_1$ and the $4c_2$ sites, respectively. For Ho^{3+}, the splitting between the ground state and excited singlet levels is only about 1 meV for the $4c_1$ site, and smaller than the computational accuracy of 0.3 meV for the $4c_2$ site (Fig. 3).

The magnetization ellipsoid can be determined from our model by calculation of the expected magnetic moment along the three crystallographic axes. The ground state doublet is considered in the case of Dy. In the case of Ho it was assumed that the first excited state is equally populated. The calculated moments, shown in Table I, of both the Ho and Dy materials have an anisotropy, with the moment on the $4c_1$ site lying predominantly along the c axis and the moment on the $4c_2$ lying along the b axis. Therefore, the fits indicate a strong Ising anisotropy in both materials.

B. Magnetic structure refinement

In order to experimentally determine the magnetic structure, neutron diffraction data were collected between $T = 50$ mK and 15 K for $SrDy_2O_4$ and between $T = 50$ mK and 25 K for $SrHo_2O_4$ using the diffractometer HRPT, PSI [24]. The crystalline and magnetic structures were refined

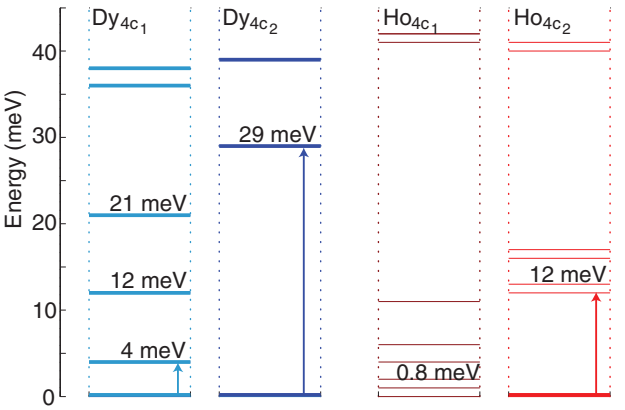

FIG. 3. (Color) The level scheme of $SrDy_2O_4$ (blue, left) and $SrHo_2O_4$ (red, right). The thick lines indicate a doublet state. The ground state of Ho_2 is a pseudodoublet.

TABLE I. Moment sizes and orientations determined from crystal-field calculations (cef), for the Dy ground state doublet and Ho pseudodoublet (pd), and determined from neutron diffraction data (exp).

	μ_B^a	μ_B^b	μ_B^c		μ_B^a	μ_B^b	μ_B^c
$Dy_{1_{cef}}$	0.7	1.5	7.7	$Dy_{2_{cef}}$	1.5	9.7	0.0
$Ho^{pd}_{1_{cef}}$	0.0	0.0	7.8	$Ho^{pd}_{2_{cef}}$	1.4	9.7	0.0
$Ho_{1_{exp}}$	0.000	0.000	6.080(3)	$Ho_{2_{exp}}$	0.000	7.740(3)	0.130(3)

simultaneously with the Rietveld refinement method implemented in FULLPROF [25], and the crystallographic structure was found to agree well with the published *Pnam* structure ($\chi^2_{Ho} = 1.869$ and $\chi^2_{Dy} = 3.866$) [3]. Below $T_N = 0.66$ K the quasi-long-range ordered magnetic structure of $SrHo_2O_4$ (the magnetic scattering is not resolution limited and single crystal measurements have shown the scattering is broad at all temperatures [7]) was found to have two types of magnetic order with different propagation vectors, $\mathbf{k}_0 = (0,0,0)$ and $\mathbf{k}_{\frac{1}{2}} = (0,0,\frac{1}{2})$ ($\chi^2 = 9.48$). These positions correspond to the two different components of the diffuse scattering. The $\mathbf{k}_0$ order is described by the *Pna'm* Shubnikov group with moments that are antiferromagnetically aligned along the *c* axis. The moment size is $6.080(3)\mu_B$ on the first site and $0.130(3)\mu_B$ on the second site, in good agreement with Ref. [26].

The $\mathbf{k}_{\frac{1}{2}} = (0,0,\frac{1}{2})$ component of the magnetic order consists of moments with a magnitude of $7.740(3)\mu_B$ along the *b* axis, which propagate in an up-up-down-down configuration along the chain. The moments of the atoms described by the $\mathbf{k}_{\frac{1}{2}}$ order are, therefore, ferromagnetically aligned within the unit cell *n* and antiparallel in the $n+1$ unit cell. Each type of order is predominantly associated with only one of the crystallographic sites, which we can uniquely assign due to the local anisotropy found from the crystal-field calculations: The $\mathbf{k}_0$ order condenses on the $4c_1$ site and $\mathbf{k}_{\frac{1}{2}}$ order on the $4c_2$ site (Fig. 4).

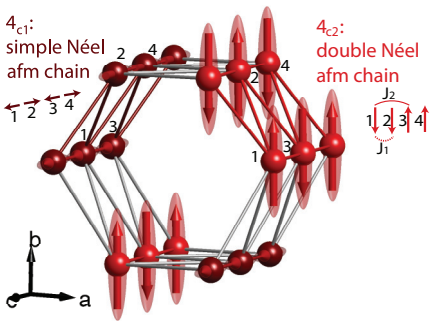

FIG. 4. (Color) Refined magnetic structure of $SrHo_2O_4$. The moments on the Ho_{c_1} sites are aligned with the *c* axis and are ferromagnetic along the rungs and antiferromagnetic between the rungs. The moments on the Ho_{c_2} sites lie along the *b* axis, and form an up-up-down-down structure along the chains.

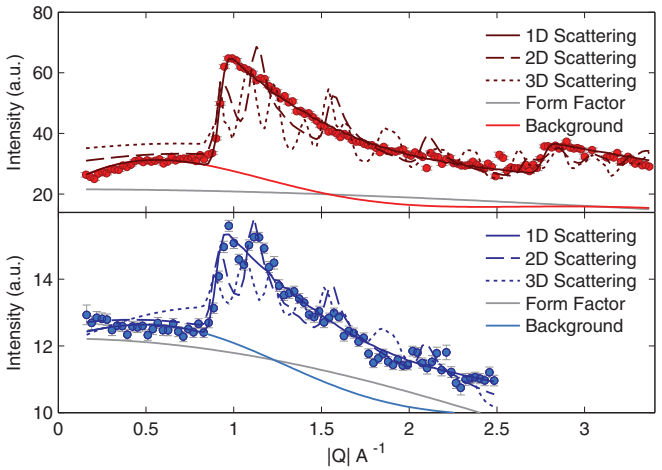

FIG. 5. (Color) Diffuse neutron scattering observed in $SrHo_2O_4$ and $SrDy_2O_4$ at 0.8 and 0.05 K, respectively. The sharp features are best fitted by a model of 1D scattering. The low temperature diffuse scattering in $SrDy_2O_4$ has an intensity reduced by approximately a factor of 10 due to the strong absorption of the sample; the first maximum in both materials is sharp and is found at $\mathbf{Q} = [0\ 0\ n + 0.5]$.

C. One-dimensional correlations

Prior to the condensation of three-dimensional (3D) order, $SrHo_2O_4$ displayed a distinctive diffuse scattering pattern. Furthermore, $SrDy_2O_4$ was found not to develop 3D magnetic order to $T = 0.05$ K, but instead presented a similar diffuse pattern. The scattering, in both the samples, has a sharp feature, found at $Q_{Ho} = 0.95$ Å^{-1} and $Q_{Dy} = 0.93$ Å^{-1} close to the position of the respective [0 0 0.5] magnetic Bragg peaks (Fig. 5). $SrHo_2O_4$ has several of these features and the maxima correspond to wave vector $\mathbf{Q} = [0\ 0\ n + 0.5]$. The features are nearly vertical on the low-$|Q|$ side and decay slowly on the high-$|Q|$ side, which is reminiscent of the powder diffraction signature of 1D correlations [27].

In order to analyze the diffuse magnetic scattering, the high temperature nuclear scattering (with a Gaussian background subtraction) was subtracted from the low temperature data ($T_{Ho} = 0.8$ K, $T_{Dy} = 0.05$ K) to leave only the diffuse and paramagnetic scattering. The data were modeled by a combination of the following: a straight line, to capture the paramagnetic scattering; a damped sine wave, to describe the scattering from short-range correlations; and a powder averaged model of reciprocal space, with scattering centered at $\mathbf{Q} = [0\ 0\ n + 0.5]$ and a "peak width" that can be controlled in order to generate 1D, 2D, and 3D scattering patterns. All components are multiplied by the magnetic form factor and their ratio refined to give the best fit to the data.

The best fit to the Ho data ($\chi^2 = 5.4$) was given by a model with intensity that was infinitely wide in the *h* and *k* directions and with a width of 0.033 reciprocal lattice units (r.l.u.) in the *l* direction, which gives a correlation length of 106 Å for the magnetic correlations along the *c* axis (see Fig. 5). The 2D model with a "peak width" of infinity, 0.1 r.l.u., and 0.033 r.l.u. in the *h*, *k*, and *l* directions gave $\chi^2 = 57.0$, and the 3D model with "peak widths" of 0.1 r.l.u. in *h* and *k* and 0.033

r.l.u. in l gave a $\chi^2 = 144.7$, underscoring the low dimensional nature of the scattering. The sine wave background was found to give a large amount of intensity centered $Q = 0.567$ Å^{-1}, close to the position of the $\mathbf{Q} = [010]$ Bragg peak, $Q = 0.528$ Å^{-1}, and indicates simultaneous short-range 3D magnetic correlations, which are not in a $[hkn + 0.5]$ plane. Assuming that the one-dimensional contribution to the diffuse scattering is from one site only, the integrated intensity of the scattering gives a moment size of $7.7(9)\mu_B$, equivalent to the size of the ordered moment found from the refinement of the ordered phase.

The best fit to the Dy data ($\chi^2 = 7.3$) was found with a scattering model that was 0.031 r.l.u. wide in the l direction, which corresponds to a correlation length of 112 Å along the c axis. The 2D and 3D models gave a χ^2 of 10.3 and 22.5, respectively. Due to the substantial absorption of natural Dy only the region $Q < 2.5$ Å^{-1} was included in the fit. The sine wave background suggests a slight development of correlations with a maximum at $Q = 0.582$ Å^{-1}, but the intensity is much less significant than that found in $SrHo_2O_4$, consistent with a much weaker tendency to long-range order in $SrDy_2O_4$ compared to $SrHo_2O_4$.

III. DISCUSSION

The diffuse scattering indicates that 1D magnetic correlations are found in both of these materials, and that in $SrHo_2O_4$ this coexists with short-range 3D correlations. The 1D magnetic correlations can be understood to be dominated by interactions along the c axis, and the interchain interaction to be extremely weak, to allow the 1D state. Finally, because the scattering lies in the $\mathbf{Q} = [hkn + 0.5]$ planes, the local order within the chains must be antiferromagnetic and similar to the magnetic order found below T_N in $SrHo_2O_4$.

The up-up-down-down, $\mathbf{k}_{\frac{1}{2}}$ magnetic structure is equivalent to that expected for a finite Ising chain when $J_2/J_1 > 1/2$ [10,11]. Our refinement of the $\mathbf{k}_{\frac{1}{2}}$ magnetic structure, combined with the evidence for the 1D nature of the correlations on the $4c_2$ site and the strong anisotropy, determined from the crystal field, all indicate that the moments on the $4c_2$ chain of Ho atoms, and by implication the $4c_2$ Dy atoms, are described by an Ising J_1-J_2 chain.

Recent magnetization measurements find a $\frac{1}{3}$ plateau when a magnetic field is applied along the b axis [5], i.e., parallel to the spins within the $4c_2$ up-up-down-down chains, and perpendicular to the spins on the $4c_1$ sites. The plateau is predicted within the Ising J_1-J_2 model, and the observation strongly supports the conclusion that $SrHo_2O_4$ and $SrDy_2O_4$ can be described as a classical Ising J_1-J_2 chain. The plateau corresponds to an up-up-down magnetic structure, which precedes a ferromagnetic phase in the $S = \frac{1}{2}$ model, or an incommensurate phase followed by a ferromagnetic phase in the classical model [10,12].

The crossover to the plateau region in $SrHo_2O_4$ and $SrDy_2O_4$ is $H = 0.59$ and 0.16 T and to the saturated phase at $H = 1.2$ and 2.03 T, respectively [5], which gives $J_2/J_{1\mathrm{Ho}} = 1.95$ and $J_2/J_{1\mathrm{Dy}} = 0.628$. The nearest- and next-nearest-neighbor interactions are thus strongly competing, locating the magnetism of the zigzag chains in the limit of $J_2/J_1 > \frac{1}{2}$. The findings strongly suggest that $SrDy_2O_4$ is a model system for the classical Ising J_1-J_2 chain close to its quantum critical point, and the emergence of the 1D magnetic correlations is the result of strong spin anisotropies and of frustrated interchain interactions.

The spin anisotropy leads to the emergent 1D magnetic physics in these materials as the magnetic moments on neighboring chains are, for the most part, orientated perpendicular to each other. Symmetric exchange, therefore, cannot induce interchain correlations. Furthermore, our symmetry analysis of the allowed Dzyaloshinskiy-Moriya (DM) interactions and calculation of the dipolar interactions show that both favor interchain order that is incompatible with the up-up-down-down structure found within the J_1-J_2 model, as any structure that is favored in the nth cell is unfavorable in the antiparallel $(n + 1)$th cell. Overall the materials can be understood as having a dimensional reduction due to the spin anisotropy and incompatible local chain order.

The dipolar interaction cannot be ruled out as a contribution to the magnetic order within the chain, as the order found in the legs of both the up-down-up-down chain and up-up-down-down minimizes the dipolar energy with respect to the local anisotropy. The antiferromagnetic order of the frustrated up-up-down-down structure, however, leads to self-shielding and hence, in this chain, only the local dipolar interactions are significant and the interaction strength J can be considered a combination of exchange and dipolar contributions [1,28]. The difference in the behavior of $SrHo_2O_4$ and $SrDy_2O_4$ underscores that the dipolar interactions alone cannot describe the physics in these materials.

If we take the values for the interactions found above, it is clear why $SrHo_2O_4$ has a higher tendency to magnetic order than $SrDy_2O_4$: The J_2/J_1 is much larger for $SrHo_2O_4$ than for $SrDy_2O_4$ so that fewer ground state fluctuations can be expected in $SrHo_2O_4$. In fact, J_2/J_1 for $SrDy_2O_4$ puts this material close to the quantum critical point of the J_1-J_2 chain.

IV. CONCLUSION

In summary, we determined the spin anisotropies in $SrHo_2O_4$ and $SrDy_2O_4$ by a fit of the crystal-field excitations, and revealed the defining features of the magnetic Hamiltonian of these two materials. We conclude that the spin physics in these materials is dominated by emergent 1D correlations and are described by the J_1-J_2 Ising chain model. This now makes it possible to study this important model system, including its excitations, in its classical limit in more detail.

ACKNOWLEDGMENTS

A.D.B. received support from the Natural Sciences and Engineering Research Council of Canada (Canada), Fonds Québécois de la Recherche sur la Nature et les Technologies (Québec), and the Canada Research Chair Foundation. A.U. acknowledges SNCF Grant No. 20021-129970. We thank Michel Gingras for his insight into the importance of the crystal fields, Tom Fennell for critical reading and scientific wisdom, and Markus Zolliker for sample environment support.

[1] J. S. Gardner, M. J. P. Gingras, and J. E. Greedan, Rev. Mod. Phys. **82**, 53 (2010).
[2] J. E. Greedan, J. Alloys Compd. **408**, 444 (2006).
[3] H. Karunadasa, Q. Huang, B. G. Ueland, J. W. Lynn, P. Schiffer, K. A. Regan, and R. J. Cava, Phys. Rev. B **71**, 144414 (2005).
[4] O. A. Petrenko, G. Balakrishnan, N. R. Wilson, S. de Brion, E. Suard, and L. C. Chapon, Phys. Rev. B **78**, 184410 (2008).
[5] T. J. Hayes, O. Young, G. Balakrishnan, and O. A. Petrenko, J. Phys. Soc. Jpn. **81**, 024708 (2012).
[6] D. L. Quintero-Castro, B. Lake, M. Reehuis, A. Niazi, H. Ryll, A. T. M. N. Islam, T. Fennell, S. A. J. Kimber, B. Klemke, J. Ollivier *et al.*, Phys. Rev. B **86**, 064203 (2012).
[7] O. Young, A. R. Wildes, P. Manuel, B. Ouladdiaf, D. D. Khalyavin, G. Balakrishnan, and O. A. Petrenko, Phys. Rev. B **88**, 024411 (2013).
[8] C. Majumdar and D. Ghosh, J. Math. Phys. **10**, 1388 (1969).
[9] T. Morita and T. Horiguchi, Phys. Lett. A **38**, 223 (1972).
[10] F. Heidrich-Meisner, I. A. Sergienko, A. E. Feiguin, and E. R. Dagotto, Phys. Rev. B **75**, 064413 (2007).
[11] J. I. Igarashi and T. Tonegawa, Phys. Rev. B **40**, 756 (1989).
[12] K. Okunishi and T. Tonegawa, Phys. Rev. B **68**, 224422 (2003).
[13] G. Castilla, S. Chakravarty, and V. J. Emery, Phys. Rev. Lett. **75**, 1823 (1995).
[14] M. Enderle, C. Mukherjee, B. Fåk, R. K. Kremer, J. M. Broto, H. Rosner, S. L. Drechsler, J. Richter, J. Malek, and A. Prokofiev, Europhys. Lett. **70**, 237 (2005).
[15] S.-L. Drechsler, O. Volkova, A. Vasiliev, N. Tristan, J. Richter, M. Schmitt, H. Rosner, J. Málek, R. Klingeler, A. Zvyagin *et al.*, Phys. Rev. Lett. **98**, 077202 (2007).
[16] J. P. Goff, D. A. Tennant, and S. E. Nagler, Phys. Rev. B **52**, 15992 (1995).
[17] W. P. Wolf, Braz. J. Phys. **30**, 794 (2000).
[18] R. Coldea, D. A. Tennant, E. M. Wheeler, E. Wawrzynska, D. Prabhakaran, M. Telling, K. Habicht, P. Smeibidl, and K. Kiefer, Science **327**, 177 (2010).
[19] M. Matsuda and K. Katsumata, J. Magn. Magn. Mater. **140**, 1671 (1995).
[20] U. Walter, J. Phys. Chem. Solids **45**, 401 (1984).
[21] T. Cheffings, M. Lees, G. Balakrishnan, and O. Petrenko, J. Phys.: Condens. Matter **25**, 256001 (2013).
[22] S. Rosenkranz, A. P. Ramirez, A. Hayashi, R. J. Cava, R. Siddharthan, and B. S. Shastry, J. Appl. Phys. **87**, 5914 (2000).
[23] A. Uldry, F. Vernay, and B. Delley, Phys. Rev. B **85**, 125133 (2012).
[24] P. Fischer, G. Frey, M. Koch, M. Könnecke, V. Pomjakushin, J. Schefer, R. Thut, N. Schlumpf, R. Bürge, and U. Greuter, Physica B **276**, 146 (2000).
[25] J. Rodríguez-Carvajal, Physica B **192**, 55 (1993).
[26] O. Young, L. Chapon, and O. Petrenko, J. Phys.: Conf. Ser. **391**, 012081 (2012).
[27] R. Jones, Acta Crystallogr. **2**, 252 (1949).
[28] L. Savary, K. A. Ross, B. D. Gaulin, J. P. C. Ruff, and L. Balents, Phys. Rev. Lett. **109**, 167201 (2012).